Talanta 221 (2021) 121452

Contents lists available at ScienceDirect

Talanta

journal homepage: www.elsevier.com/locate/talanta

# HER2 breast cancer biomarker detection using a sandwich optical fiber assay

Médéric Loyez [a,*], Maxime Lobry [b], Eman M. Hassan [c,d], Maria C. DeRosa [c], Christophe Caucheteur [b], Ruddy Wattiez [a]

[a] Proteomics and Microbiology Department, University of Mons, Place Du Parc 20, 7000, Mons, Belgium
[b] Electromagnetism and Telecommunications Department, University of Mons, Bld. Dolez 31, 7000, Mons, Belgium
[c] Institute of Biochemistry, Carleton University, 1125 Colonel By Drive, Ottawa, Ontario, K1S 5B6, Canada
[d] Metrology Research Centre, National Research Council Canada, Ottawa, Ontario, K1A 0R6, Canada

ARTICLE INFO

*Keywords:*
Optical fiber
Breast cancer diagnosis
HER2
Biomarker
Aptamers
Surface plasmon resonance

ABSTRACT

Optical fiber-based surface plasmon resonance (OF-SPR) sensors have demonstrated high versatility and performances over the last years, which propelled the technique to the heart of numerous and original biosensing concepts. In this work, we contribute to this effort and present our recent findings about the detection of breast cancer HER2 biomarkers through OF-SPR optrodes. 1 cm-long sections of 400 μm core-diameter optical fibers were covered with a sputtered gold film, yielding enhanced sensitivity to surface refractive index changes. Studying the impacts of the gold film thickness on the plasmonic spectral response, we improved the quality and reproducibility of the sensors. These achievements were correlated in two ways, using both the central wavelengths of the plasmon resonance and its influence on the bulk refractive index sensitivity. Our dataset was fed by additional biosensing experiments with a direct and indirect approach, relying on aptamers and antibodies specifically implemented in a sandwich layout. HER2 biomarkers were specifically detected at 0.6 μg/mL (5.16 nM) in label-free while the amplification with HER2-antibodies provided a nearly hundredfold signal magnification, reaching 9.3 ng/mL (77.4 pM). We believe that these results harbinger the way for their further use in biomedical samples.

## 1. Introduction

Receptor tyrosine-kinase HER2 (ErbB2) is member of the human epidermal growth factor receptor (EGFR) family. Its overexpression plays an important role in the progression and development of aggressive breast cancers [1]. HER2 receptors are crucial to cell growth, survival and differentiation. Each receptor consists of an extracellular ligand-binding domain, a transmembrane domain and a tyrosine-kinase domain. While the ligand is binding, receptors are activated by auto- and cross-phosphorylation. However, there is no known ligand for HER2, which does not need to be bound to be activated. Indeed, HER2 is the preferential dimerization partner among all the tyrosine kinase family. Once activated, it induces downstream activations. Two cell signalization pathways are mainly targeted: the phosphoinositide 3-kinase/Protein Kinase B (PI3K/AKT) [2] and the RAF/MEK/MAPK pathways [3]. This leads to a higher proliferation, cell-cycle progression, etc. Moreover, cancer cases where these receptors are expressed can be treated with molecules such as the trastuzumab, or more generally tyrosine kinase inhibitors (TKIs), limiting the activation of these pathways and regulating the proto-oncogenic system [4]. HER2+ patients are suitable for trastuzumab therapy but as it is expensive and associated with risks for cardiac toxicity, the risks for trastuzumab in HER2-patients outweigh its benefits. HER2 detection is therefore useful to determine the prognosis and therapy for breast cancer [5].

Our study relies on Surface Plasmon Resonance (SPR) optical fiber sensors to detect HER2 proteins while monitoring binding events in real time. Nowadays, the majority of commercial SPR systems (e.g. Biacore from GE Healthcare) are fully automated and adapted for the use of biochips and microfluidics, but are limited to laboratory use [6]. The transposition of the SPR principle to optical fibers therefore brings many practical assets such as miniaturization, flexibility, and remote control, among others [7,8]. It has already proven high potential for the detection of biomarkers in tissues [9,10], detection of circulating cells [11], or

* Corresponding author.
*E-mail address:* mederic.loyez@umons.ac.be (M. Loyez).

https://doi.org/10.1016/j.talanta.2020.121452
Received 9 June 2020; Received in revised form 17 July 2020; Accepted 22 July 2020
Available online 30 July 2020

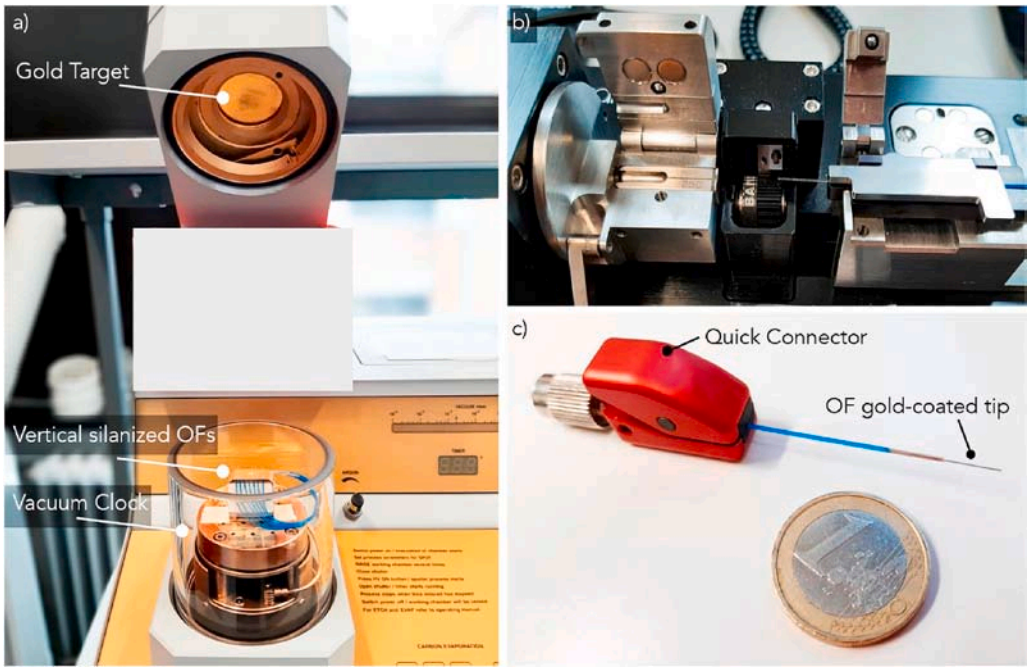


**Fig. 1.** (a) Picture of the gold sputter-coater. Optical fibers were placed vertically inside the vacuum chamber. The quartz microbalance is at the level of the lower stage in the vacuum clock. (b) Picture of the optical fiber cleaving machine, to cut the 400 μm-diameter optical fibers. (c) Picture of the OF-SPR probes inside a quick connector. (For interpretation of the references to colour in this figure legend, the reader is referred to the Web version of this article.)

the identification of analytes of interest in body fluids [12–14].

Many optical fiber SPR configurations exist. Among these, one of the most documented and straightforward technique is the use of multimode unclad optical fibers [15]. Indeed, by depositing a thin gold film directly onto the exposed core of an optical fiber, it is possible to reach the SPR excitation, consequently yielding improved surface refractive index sensitivity. This was already demonstrated in the nineties while Jorgenson and Yee combined the optical fiber technology with SPR [16]. Long Period Fiber Gratings (LPFGs – refractive index modulations photo-imprinted in the core of single-mode optical fibers with a typical period of a few hundreds of nanometers and allowing to couple light to the cladding in the forward direction) [17,18], U-bent fibers [19,20] have also shown high-resolution biosensing features. Another possibility is the use of Tilted Fiber Bragg Gratings (TFBGs – short period of around 500 nm refractive index modulations slightly angled with respect to the perpendicular to the optical fiber axis that couple light to the cladding in the backward direction) [21–23], a domain to which we have largely contributed by the past [24–26].

In this paper, we have studied the spectral features of unclad optical fibers to evaluate and optimize their sensitivity against HER2 proteins, using both label-free and amplified response through antibodies [27].

The plasmonic unclad fiber approach (OF-SPR) consists of a white light source (400–850 nm) and a spectrophotometer both connected to the plasmonic probe by a bifurcated optical wire [28]. The light is guided to the fiber tip and is then reflected back to the spectrometer. The selected biosensing strategy consists of thiolated anti-HER2 aptamers directly bound to thin gold film deposited on the optical fiber surface. A signal amplification was also conducted with additional anti-HER2 antibodies after the binding on the biosensor surface. A thorough study of the SPR responses combining the thickness of the gold layer and the refractive index sensitivity was also performed to optimize our experimental protocols and to boost their limits of detection.

## 2. Material and methods

### 2.1. Materials

Phosphate Buffer Saline (PBS) came from Thermo Fisher Scientific (Merelbeke, Belgium). 6-mercapto-1-hexanol was purchased from Sigma Aldrich (Merck, Darmstadt, Germany). Thiolated-aptamers against HER2 proteins were synthesized at Carleton University with sequence ref. He_A2_3 [29]. The HER2 protein (recombinant human protein ErbB2, 116 kDa) came from Abcam (ab60866). Anti-HER2 antibodies come from Bioss Antibodies (BOSSBS-2896R from VWR). Lateral flow assay was performed to ensure the interaction with this commercial protein and the synthesized aptamer. FT400UMT TECS Hard Clad, 0.39 NA, Step-Index optical fiber (unclad configuration) came from Thorlabs. Standard silica SMF-28 optical fiber (TFBG configuration) came from Corning. Vytran compact fiber cleaver, the 400 μm Y-bundle FC/PC and BFT1 connectors came from Thorlabs. Halogen white light source and HR4000 spectrometer came from OceanOptics. (Trimethylsilyls)-3-propanethiol came from VWR.

### 2.2. Gold-coated optical fibers

The OF-SPR sensors were manufactured using FT400 Step-Index multimode fiber with a core diameter of 400 μm (Thorlabs). The core is in silica and is surrounded a TECS cladding of 25 μm. A hard cladding is also present around the optical fiber, and is around 300 μm thick. The optical fibers presents a numerical aperture of 0.39. Pieces of OF were cut, and a section of 4 cm was stripped at the fiber end using a dedicated clamp. The stripped part of the OF was then immersed in acetone to remove the TECS hard polymer cladding, and cleaned manually by a cloth soaked in acetone until total removal of cladding remains. A microscopic inspection with an optical microscope was performed to ensure that the cladding was perfectly removed on the entire fiber tip. The optical fibers were then cut using a Vytran compact fiber cleaver (Thorlabs), to obtain 1 cm unclad sensing areas, and cut on the other side to connect the fiber. Final probe lengths of about 5 cm were used to keep fiber straight during measurements.

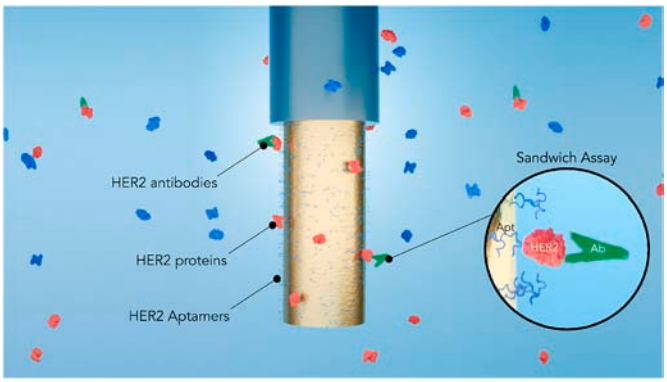


**Fig. 2.** Artistic view of the gold coated unclad fiber used to specifically detect HER2 molecules (in red) through SPR, with antibodies amplification in a sandwich configuration (in green). Thiolated aptamers are immobilized on the gold surface to target HER2. (For interpretation of the references to colour in this figure legend, the reader is referred to the Web version of this article.)

The optical fiber tips were then cleaned into piranha solution ($H_2SO_4$ and $H_2O_2$ 3:1) and silanized in methanol using 1% solution of (trimethylsilyls)-3-propanethiol during 15 min at room temperature, (RT). The optical fibers were then dried overnight at RT and mounted on a holder for a single gold sputter deposition, which was performed vertically (Fig. 1).

The deposition was performed under vacuum ($\sim 10^{-4}$ mbar) with argon, into a LEICA EM SCD500 sputter-coater with integrated quartz microbalance.

### 2.3. Biofunctionalization

The gold-coated optical fibers were biofunctionalized with anti-HER2 ssDNA aptamers directly linked onto the gold surface with the aim to specifically detect HER2 proteins. These aptamers were selected by the Systematic Evolution of Ligands by EXponential enrichment (SELEX) [29]. Thiolated anti-HER2 aptamers were synthesized with a MerMade 6 automated DNA synthesizer (BioAutomation, USA) through phosphoramidite chemistry leading to the following ssDNA aptamer sequence: 5′-TCT AAA AGG ATT CTT CCC AAG GGG ATC CAA TTC AAA CAG 6 S–S-3'. This step was performed using DNA bases and thiol-modifiers from Glen Research (Sterling, VA, USA). Before their immobilization, thiol-modified aptamers were resuspended in TE buffer (Tris-ethylenediaminetetraacetic acid) 100 μM from Base Pair Biotechnologies and diluted 1:1 v/v with TCEP (Tris (2-carboxyethyl) phosphine) solution from Base Pair Biotechnologies to be reduced at 90 °C for 5 min. The aptamers were then diluted with PBS, pH 7.2 to reach a working concentration of 10.24 μM. Each gold-coated fiber was then immersed in small volume (300 μL) of aptamers solution for the immobilization step during 1h in PBS at RT. Blocking was performed during 30 min using 6-mercapto-1-hexanol 5 mM in PBS.

### 2.4. Biosensing experiments and signal analysis

The functionalized probes were tested in PBS, using target breast cancer biomarkers (HER2) at different concentrations. To confirm the specificity of the sensors, they were also put in contact with non-target cytokeratin-17 proteins (CK17) which are lung cancer biomarkers [30]. The sensors were connected to a white light source (halogen lamp), and a spectrometer (HR4000 from OceanOptics) with a resolution of 0.1 nm. They were both connected through a bifurcating optical cable. After the detection of HER2 at low concentrations, anti-HER2 antibodies were used at a working concentration of 20 μg/mL as signal enhancers to lower the limit of detection of the device (Fig. 2). The binding of antibodies onto HER2 proteins already caught on the surface will enhance the signal change by a mass effect. Using this sandwich assay (aptamers-HER2-antibodies), we therefore enhance the SPR shift.

The amplitude spectrum released from the OF-SPR setup results in a dip-curve (Fig. 3). The SPR dip quality (full width at half maximum: FWHM, and intensity: depth) is influenced by the mode propagation angle and the number of reflections occurring inside the fiber [31–33]. Given this, several lengths between 0.5 cm and 2.0 cm were tested for the optical fiber optrodes and it turns out that the best performances were obtained for 1 cm long (±10%) unclad section. The position of the resonance, its FWHM and the spectrum flaring were the three parameters followed to qualify the sensing behavior. Classical refractive index sensitivities achieved with unclad multimode fibers are reported to be between roughly 1500 nm/RIU and 2500 nm/RIU in literature, depending on the metal deposition and the selected structures, sizes, etc. [34,35].

The optimization of the gold deposition and optical fibers structures were studied through refractometric measurements, conducted with LiCl dilutions calibrated using a refractometer with a precision of $10^{-4}$ RIU (Reichert). The SPR-curves were normalized individually by dividing the acquired data by its maximum amplitude, to obtain comparable spectra from 0 to 1 as a normalized power-scale. The minimum of the SPR-curves was tracked to calculate the sensitivity. The signal analysis was performed using our own MATLAB script for automated monitoring of the response.

## 3. Experimental results

### 3.1. Refractometry

The first refractometric experiments were conducted on 40 optical fibers to ensure the further production of reliable probes and to

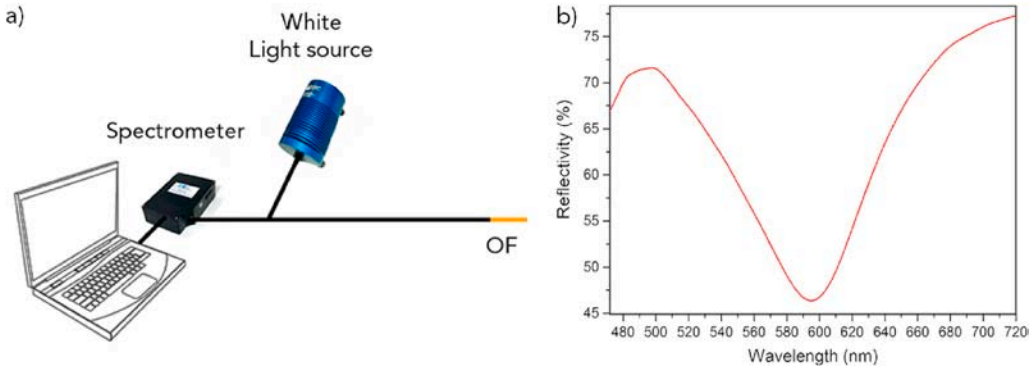


**Fig. 3.** (a) Scheme of the optical fiber probe connected to a spectrometer and a white light source (480–720 nm). The device is portable and can be connected to a laptop. (b) Gaussian SPR curve obtained with the gold-coated OF in PBS. (For interpretation of the references to colour in this figure legend, the reader is referred to the Web version of this article.)

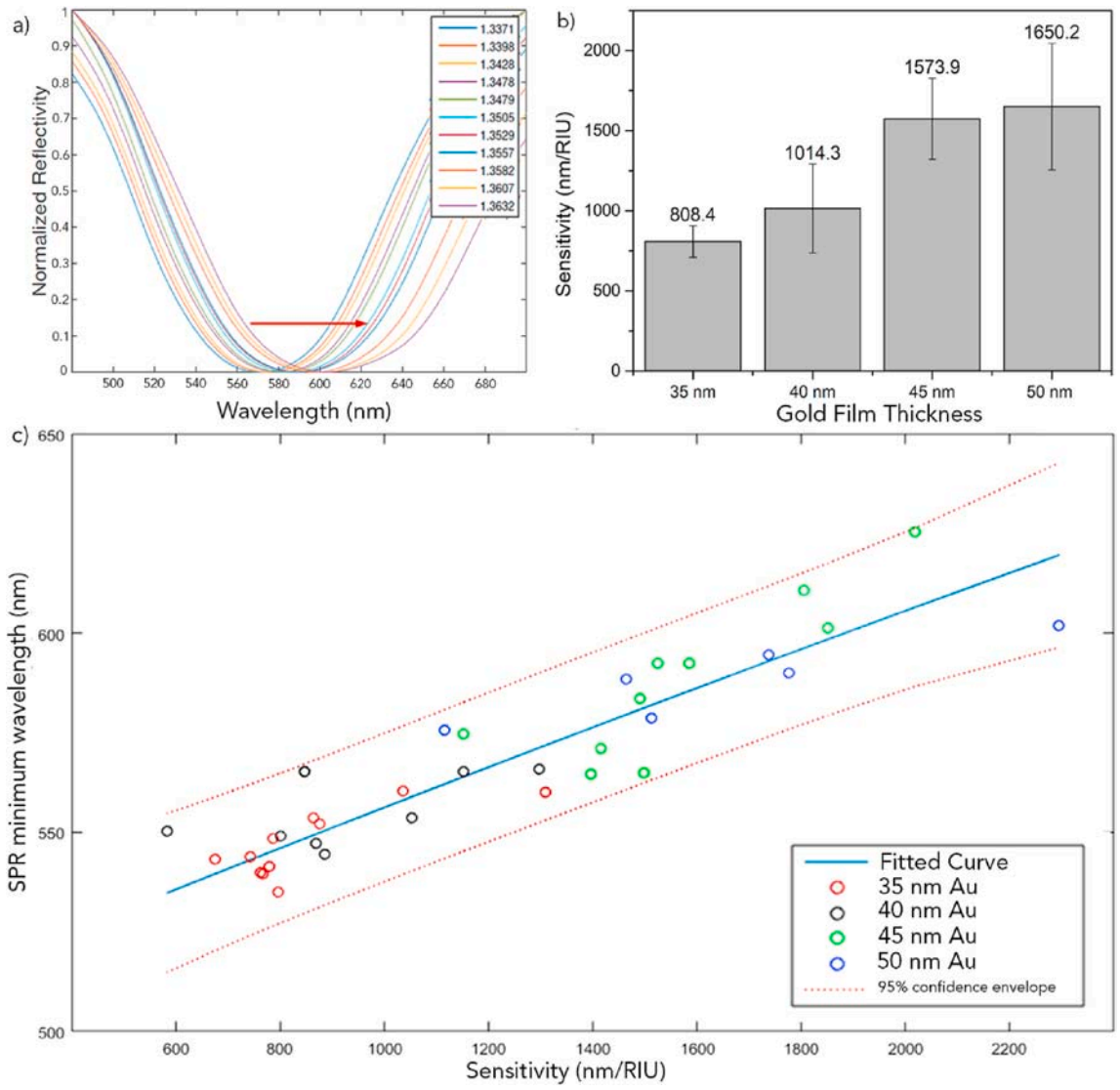


**Fig. 4.** (a) Evolution of the normalized spectrum in growing LiCl concentrations (RI change). (b) Evolution of the sensitivity as function of the gold film thickness (mean ± sd). (c) Evolution of the SPR lambda 0 wavelength in PBS with different probes coated with growing gold film thicknesses (Fitted curve and 95% confidence envelope). (For interpretation of the references to colour in this figure legend, the reader is referred to the Web version of this article.)

**Table 1**
Experimental sensitivities obtained with different gold film thicknesses.

| Fiber number | Sensitivity with 35 nm Au (nm/RIU) | Sensitivity with 40 nm Au (nm/RIU) | Sensitivity with 45 nm Au (nm/RIU) | Sensitivity with 50 nm Au (nm/RIU) |
|---|---|---|---|---|
| 1 | 1035.85 | 801.07 | 1416.11 | 1464.38 |
| 2 | 674.45 | 687.16 | 1395.18 | 1775.73 |
| 3 | 787.31 | 1059.91 | 1497.49 | 1738.65 |
| 4 | 742.16 | 925.34 | 1152.83 | 1512.28 |
| 5 | 761.69 | 869.45 | 1851.78 | 2295.65 |
| 6 | 863.67 | 1298.02 | 2018.03 | 1114.56 |
| 7 | 778.86 | 886.22 | 1490.92 | – |
| 8 | 767.76 | 1150.66 | 1525.78 | – |
| 9 | 796.76 | 1619.09 | 1806.18 | – |
| 10 | 875.78 | 846.78 | 1585.58 | – |
| mean | 808.43 | 1014.37 | 1573.99 | 1650.21 |
| sd | 98.29 | 277.45 | 253.36 | 395.13 |

characterize their sensitivity to surrounding medium changes. To enhance the SPR quality, different parameters were optimized. Indeed, it is well known that the gold layer has to reach a sufficient thickness leading to a deep resonance but if the latter becomes too thick, it also yields lowered excitation of surface plasmons. Moreover, the quality of the cleaving at the end of the fiber tip appears to play an important role on the symmetry of the obtained SPR curve [32,36].

Among the thicknesses able to provide strong SPR resonances with our probes, we have tested 35, 40, 45 and 50 nm coated probes (values obtained from the built-in quartz microbalance, with a reliability of ±1 nm) using refractometry. The fibers were successively immersed in growing LiCl concentrations to obtain calibration curves (Fig. 4a). The wavelength of the minimum of the SPR was used to determine the sensitivity of the fibers, as reported in Table 1.

The experimental results show growing sensitivities following the increase of the gold film but also with an increased variability starting from 50 nm gold thickness (Fig. 4b). Similar conclusions about the increase in sensitivity related with the increase of gold thickness were pointed out on a glass prism pre-covered with a chromium film [36]. Some investigations were also initiated on optical fibers over the last decade to deal with the influence of metal films on SPR [37–39]. It is pointed out that the configuration used is highly tuning the sensitivity of the method [40].

In this work, it was not possible to obtain deep SPR responses neither

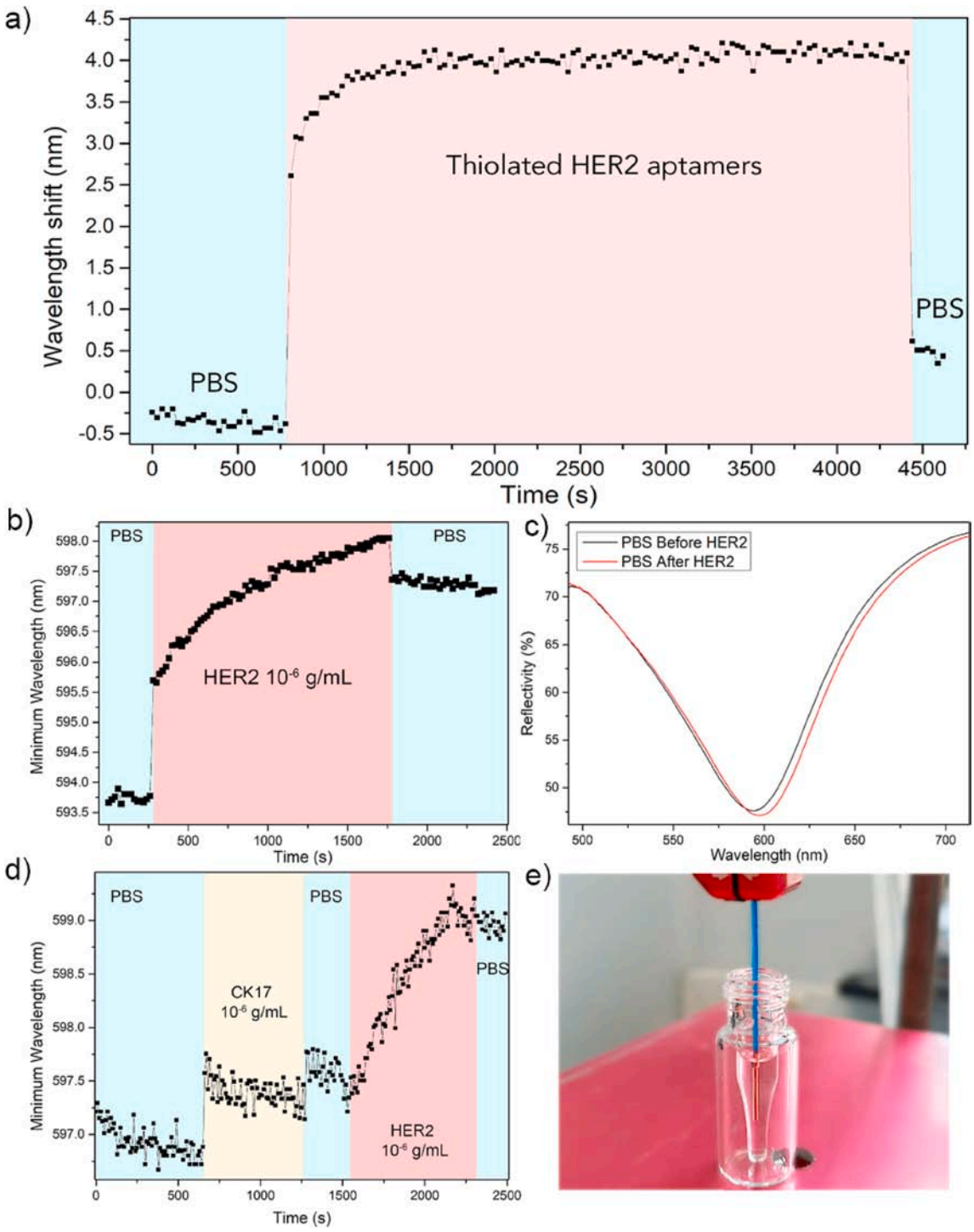


**Fig. 5.** (a) Evolution of the minimum of the SPR curve in PBS, reduced anti-HER2 thiolated ssDNA aptamers, and PBS after the immobilization. (b) Evolution of the SPR-dip minimum in PBS, HER2 proteins 1 μg/mL, and PBS after the detection. (c) OF-SPR curves before and after the immersion in HER2, in PBS. (d) Selectivity test with CK17 proteins before detection of HER2 proteins. (e) Picture of the experimental setup with the probe inserted in a 125 μL vial for the HER2 protein detection. The position of the fiber is managed to stay in the center without contact with the vial.

below 35 nm nor beyond 50 nm. It was noticed that for a gold thickness of 50 nm, only 60% of the optrodes featured a correct SPR resonance, weakening the reproducibility of the deposition process. It has also to be mentioned that the quartz microbalance is located at 4 cm from the top of the optical fibers that probably receive a slight gold gradient along their longitudinal axis as they are placed vertically in the sputtering chamber. It is therefore challenging to determine the actual thickness of the deposited film, as it is not exactly the same at the tip and on the sides of the fiber, even if precision measurements such as atomic force microscopy (AFM) can deal with the thickness evaluation for uniform films.

We have also noticed that the gold thickness influences the wavelength position of the SPR resonance ($\lambda_0$) and subsequently its refractometric sensitivity. $\lambda_0$ is the wavelength corresponding to the central wavelength (location of the minimum) when the optrode is immersed in PBS, a solution of refractive index equal to 1.3367 ± 0.0002 (calculated

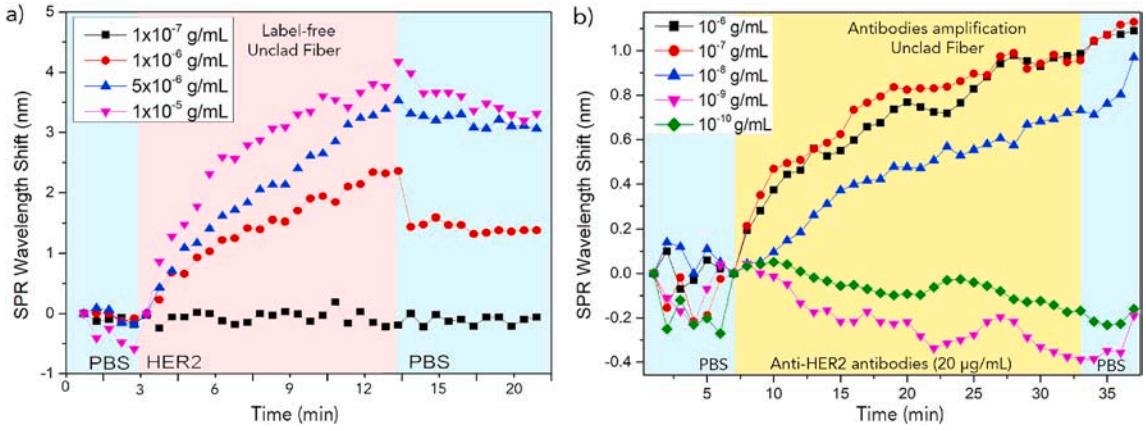


**Fig. 6.** (a) Evolution of the SPR-dip minimum in PBS, HER2 proteins, and PBS after the immersion in HER2 solution. (b) Evolution of the SPR-dip minimum in PBS, in antibodies (anti-HER2), and in PBS after amplification. Each curve represents one probe per test.

at a narrow ray of yellow light from glowing sodium, at 589 nm). The results of this comparison between sensitivity and $\lambda_0$ are shown in Fig. 4c. A linear evolution between $\lambda_0$ and sensitivity can be noticed, with a reliability envelope at 95%. Moreover, this graph presents also all the gold thicknesses tested.

Considering these results, the biosensing experiments were performed using 45 nm gold-coated 1 cm-long optrodes for which $\lambda_0$ is higher than 585 nm.

### 3.2. Biofunctionalization and HER2 detection

The HER2-aptamers immobilization was recorded in real time by tracking wavelength shifts in the spectral response. Our observations indicate a sudden wavelength shift when moving from PBS to the aptamers solution. This results from a slight refractive index change between both solutions. A progressive wavelength shift ($1.5 \pm 0.5$ nm) is then measured in the aptamers solution, indicating that aptamers are well grafted on the gold surface after 1 h (Fig. 5a). In order to avoid non-specific adsorption, a blocking step using 6-mercapto-1-hexanol 5 mM was finally performed during 30 min in PBS at room temperature.

Concerning the ability to detect target proteins, the sensitivity for HER2 was first tested using a 1 µg/mL concentration. The fibers were monitored until stabilization in PBS, then in HER2 1 µg/mL and back into PBS (Fig. 5b and c). The response demonstrates strong interactions between proteins and the optical fiber surface, remaining before/after its immersion in PBS. The selectivity for HER2 was also verified using non-target CK17 protein at 1 µg/mL in PBS, as a negative control (Fig. 5d). No significant shift was observed in this protein solution, and the fiber kept its integrity and ability to anchor the HER2 targets at 1 µg/mL after this test. A negative control performed with a non-functionalized unclad fiber immersed in different proteins is presented in Supp. Information, Fig. S1 to verify the absence of non-specific adsorption. The interrogation setup allows to perform the detection in small vials of only 125 µL, limiting the need for important sampling (Fig. 5e). The length of the optical fibers (cladding part) can also be adjusted as a function of the target application.

### 3.3. Sandwich assay using antibodies

A first range of selected concentrations between $10^{-12}$ g/mL (~8 fM) and $10^{-6}$ g/mL (~8 nM) showed a signal response beginning at $10^{-6}$ g/mL (~8 nM) for this label-free configuration (Fig. 6a). Experiments were extensively conducted around this concentration and at higher concentrations up to 10 µg/mL to obtain a more detailed overview of the detection performances. Our experimental data can be correlated with literature where similar performances were obtained in label-free strategies [41].

**Table 2**
Performance indicators calculated from experimental values.

| Performance Indicator | Experimental value |
|---|---|
| $Sensitivity = \frac{\Delta\lambda}{\Delta\ analyte}$ | $Sensitivity = \frac{1.5\ nm}{8.6\ nM} = 0.17$ nm/nM |
| $FOM = \frac{Sensitivity}{FWHM}$ | $FOM = \frac{0.17}{100\ nm} = 0.0017$ |
| $Q\ Factor = \frac{\lambda_0}{FWHM}$ | $Q\ Factor = \frac{600\ nm}{100\ nm} = 6$ |
| $LOD_{Label-free}$ *reported on experimental calibration curve*(3σ in blank) | $LOD_{Label-free} = 6.6 \times 10^{-7}$ g/mL |
| $LOD_{Amplified}$ reported on experimental calibration curve(3σ in blank) | $LOD_{Amplified} = 9.3 \times 10^{-9}$ g/mL |

After the label-free detection of HER2, the optical fibers were washed into PBS and immersed in anti-HER2 antibody solution (20 µg/mL) to improve their detection threshold. Interrestingly, Fig. 6b shows this bio-amplification, increased by a factor 100, reaching $10^{-8}$ g/mL (~86 pM) for the limit of detection in our experimental conditions.

### 3.4. Performances indicators

We tried to fairly estimate the performances of this unclad fiber technique, following the IUPAC recommendations (Table 2). First, the sensitivity was calculated as a ratio between the signal response and the change of target concentration. Second, the Figure of Merit (FOM) for a wavelength shift was calculated as a ratio between the sensitivity (nm) and the linewidth of the resonance, taking into account that it is easier to measure the exact location of a narrow resonance than a broad resonance. The Q-Factor for "quality factor" was calculated as a quotient between the initial wavelength of the resonance and the full width at half maximum or minimum (FWHM).

A high Q-factor indicates that FWHM is small in comparison with its central wavelength, so there is a good capability to distinguish close SRI values. A low Q-factor means that is it more difficult to use the sensor to distinguish close variations of SRI (or target concentrations). Finally, the

limit of detection was evaluated as the lowest concentration of the target which can be detected by the device, based on experimental calibration curves [41,42](Supp. Information, Fig. S2). These raw values have to be correlated with the experimental context, for the detection of HER2 proteins within 10 min and into small volumes (125 μL). The amplification of the signal makes this approach highly sensitive with a simple, point-of-care and user-friendly setup.

## 4. Conclusion and prospects

The unclad OF-SPR technique is simple to readout and call on cost-effective equipment (white light source and spectrometer). Our experiments lead to the generation of optimized surface plasmons thanks to a robust study on the influence of the gold film thickness and the central wavelength of the SPR curve on the refractive index sensitivity. These results were confirmed by multiple assays, and our dataset was improved by implementing biosensing with a direct and indirect approach targeting HER2 proteins. Target biomarkers were specifically detected at 1 μg/mL using a label-free technique while the amplification with HER2-antibodies yielded a 100x improved threshold, reaching 10 ng/mL (~86 pM). Finally, some of the standard performance indicators were calculated based on our experimental results, as fair values for their evaluation, depending on the target application.

We believe that this study, carried out on a large number of sensors, gives key elements for their future development as rapid diagnostic biosensors. Multiplexing using different fibers side by side, or using bioreceptors dropped in spots along the fiber tip are some of their many prospects which could be of interest for their use with biomedical samples.

## Author contributions

Médéric Loyez (M.L.), experiments, data analyses and writing; Maxime Lobry (M.L.), samples preparation; Eman M Hassan (E.M.H), aptamers production; Maria C. DeRosa (M.C.D.), Christophe Caucheteur (C·C.) and Ruddy Wattiez (R.W.), data analysis and project supervision.

## Declaration of competing interest

The authors declare that they have no known competing financial interests or personal relationships that could have appeared to influence the work reported in this paper.

## Acknowledgements

We warmly thank Mariel David for her help in the samples preparation. We also thank the group of Prof. Jeroen Lammertyn (MeBios, KU Leuven), for his help and feedback about the biosensing experiments.

## Appendix A. Supplementary data

Supplementary data to this article can be found online at https://doi.org/10.1016/j.talanta.2020.121452.

## Funding sources

This work was financially supported by the Fonds de la Recherche Scientifique – FNRS, with the Postdoctoral Researcher Fellowship of Médéric Loyez (Chargé de Recherches, FRS-FNRS), the Associate Researcher position of Christophe Caucheteur (FRS-FNRS) and Grant n°O001518F (EOS-convention 30467715). We acknowledge the Natural Sciences and Research Council of Canada for their funding (Discovery Grant 224070).

## References

[1] J.S. Ross, J.A. Fletcher, G.P. Linette, J. Stec, E. Clark, M. Ayers, W.F. Symmans, L. Pusztai, K.J. Bloom, The HER-2/neu gene and protein in breast cancer 2003: biomarker and target of therapy, Oncol. 8 (2003) 307–325, https://doi.org/10.1634/theoncologist.8-4-307.

[2] K. Araki, Y. Miyoshi, Mechanism of resistance to endocrine therapy in breast cancer: the important role of PI3K/Akt/mTOR in estrogen receptor-positive, HER2-negative breast cancer, Breast Cancer 25 (2018) 392–401, https://doi.org/10.1007/s12282-017-0812-x.

[3] V. Belli, N. Matrone, S. Napolitano, G. Migliardi, F. Cottino, A. Bertotti, L. Trusolino, E. Martinelli, F. Morgillo, D. Ciardiello, V. De Falco, E.F. Giunta, U. Bracale, F. Ciardiello, T. Troiani, Combined blockade of MEK and PI3KCA as an effective antitumor strategy in HER2 gene amplified human colorectal cancer models, J. Exp. Clin. Canc. Res. 38 (2019) 1–14, https://doi.org/10.1186/s13046-019-1230-z.

[4] D.L. Nielsen, M. Andersson, C. Kamby, HER2-targeted therapy in breast cancer. Monoclonal antibodies and tyrosine kinase inhibitors, Canc. Treat Rev. 35 (2009) 121–136, https://doi.org/10.1016/j.ctrv.2008.09.003.

[5] T. Doi, K. Shitara, Y. Naito, A. Shimomura, Y. Fujiwara, K. Yonemori, C. Shimizu, T. Shimoi, Y. Kuboki, N. Matsubara, A. Kitano, T. Jikoh, C. Lee, Y. Fujisaki, Y. Ogitani, A. Yver, K. Tamura, Safety, pharmacokinetics, and antitumour activity of trastuzumab deruxtecan (DS-8201), a HER2-targeting antibody–drug conjugate, in patients with advanced breast and gastric or gastro-oesophageal tumours: a phase 1 dose-escalation study, Lancet Oncol. 18 (2017) 1512–1522, https://doi.org/10.1016/S1470-2045(17)30604-6.

[6] C. Chen, J. Wang, Optical biosensors: an exhaustive and comprehensive review, Analyst 145 (2020) 1605–1628, https://doi.org/10.1039/c9an01998g.

[7] J.H. Qu, A. Dillen, W. Saeys, J. Lammertyn, D. Spasic, Advancements in SPR biosensing technology: an overview of recent trends in smart layers design, multiplexing concepts, continuous monitoring and in vivo sensing, Anal. Chim. Acta 1104 (2019) 10–27, https://doi.org/10.1016/j.aca.2019.12.067.

[8] B. Špačková, N.S. Lynn, J. Slabý, H. Šípová, J. Homola, A route to superior performance of a nanoplasmonic biosensor: consideration of both photonic and mass transport aspects, ACS Photonics 5 (2018) 1019–1025, https://doi.org/10.1021/acsphotonics.7b01319.

[9] C. Ribaut, M. Loyez, J. Larrieu, S. Chevineau, P. Lambert, M. Remmelink, R. Wattiez, C. Caucheteur, Cancer biomarker sensing using packaged plasmonic optical fiber gratings : towards in vivo diagnosis, Biosens. Bioelectron. 92 (2017) 449–456, https://doi.org/10.1016/j.bios.2016.10.081.

[10] M. Loyez, J. Larrieu, S. Chevineau, M. Remmelink, D. Leduc, B. Bondue, P. Lambert, J. Devière, R. Wattiez, C. Caucheteur, In situ cancer diagnosis through online plasmonics, Biosens. Bioelectron. 131 (2019) 104–112, https://doi.org/10.1016/j.bios.2019.01.062.

[11] M. Loyez, E.M. Hassan, M. Lobry, F. Liu, C. Caucheteur, R. Wattiez, M.C. DeRosa, W.G. Willmore, J. Albert, Rapid detection of circulating breast cancer cells using a multiresonant optical fiber aptasensor with plasmonic amplification, ACS Sens. 5 (2020), https://doi.org/10.1021/acssensors.9b02155.

[12] L. Han, T. Guo, C. Xie, P. Xu, J. Lao, X. Zhang, J. Xu, X. Chen, Y. Huang, X. Liang, W. Mao, B.O. Guan, Specific detection of aquaporin-2 using plasmonic tilted fiber grating sensors, J. Lightwave Technol. 35 (2017) 3360–3365, https://doi.org/10.1109/JLT.2016.2645233.

[13] M.S. Aruna Gandhi, S. Chu, K. Senthilnathan, P.R. Babu, K. Nakkeeran, Q. Li, Recent advances in plasmonic sensor-based fiber optic probes for biological applications, Appl. Sci. 9 (2019), https://doi.org/10.3390/app9050949.

[14] T. Guo, F. Liu, X. Liang, X. Qiu, Y. Huang, C. Xie, P. Xu, Highly sensitive detection of urinary protein variations using tilted fiber grating sensors with plasmonic nanocoatings, Biosens. Bioelectron. 78 (2016) 221–228, https://doi.org/10.1016/j.bios.2015.11.047.

[15] A.B. Socorro-Leránoz, D. Santano, I. Del Villar, I.R. Matias, Trends in the design of wavelength-based optical fibre biosensors (2008–2018), Biosens. Bioelectron. X. 1 (2019) 100015, https://doi.org/10.1016/j.biosx.2019.100015.

[16] R.C. Jorgenson, S.S. Yee, A fiber-optic chemical sensor based on surface plasmon resonance, Sensor. Actuator. B Chem. 12 (1993) 213–220, https://doi.org/10.1016/0925-4005(93)80021-3.

[17] F. Chiavaioli, F. Baldini, S. Tombelli, C. Trono, A. Giannetti, Biosensing with optical fiber gratings, Nanophotonics 6 (2017) 663–679, https://doi.org/10.1515/nanoph-2016-0178.

[18] S. Bandyopadhyay, P. Biswas, F. Chiavaioli, T.K. Dey, N. Basumallick, C. Trono, A. Giannetti, S. Tombelli, F. Baldini, S. Bandyopadhyay, Long-period fiber grating: a specific design for biosensing applications, Appl. Optic. 56 (2017) 9846, https://doi.org/10.1364/AO.56.009846.

[19] C. Christopher, A. Subrahmanyam, V.V.R. Sai, Gold sputtered U-bent plastic optical fiber probes as SPR- and LSPR-based compact plasmonic sensors, Plasmonics 13 (2018) 493–502, https://doi.org/10.1007/s11468-017-0535-z.

[20] H. Manoharan, P. Kalita, S. Gupta, V.V.R. Sai, Plasmonic biosensors for bacterial endotoxin detection on biomimetic C-18 supported fiber optic probes, Biosens. Bioelectron. 129 (2019) 79–86, https://doi.org/10.1016/j.bios.2018.12.045.

[21] Y.Y. Shevchenko, J. Albert, Plasmon resonances in gold-coated tilted fiber Bragg gratings, Opt. Lett. 32 (2007) 211–213.

[22] J. Albert, L. Shao, C. Caucheteur, Tilted fiber Bragg grating sensors, Laser Photon. Rev. (2012) 1–26, https://doi.org/10.1002/lpor.201100039.

[23] K.A. Tomyshev, E.S. Manuilovich, D.K. Tazhetdinova, E.I. Dolzhenko, O.V. Butov, High-precision data analysis for TFBG-assisted refractometer, Sensors Actuators, A Phys. 308 (2020) 112016, https://doi.org/10.1016/j.sna.2020.112016.

[24] M. Loyez, M. Lobry, R. Wattiez, C. Caucheteur, Optical fiber gratings immunoassays, Sensors 19 (2019) 2595.
[25] M. Lobry, D. Lahem, M. Loyez, M. Debliquy, K. Chah, M. David, C. Caucheteur, Non-enzymatic D-glucose plasmonic optical fiber grating biosensor, Biosens. Bioelectron. 142 (2019) 111506.
[26] T. Guo, Á. González-vila, M. Loyez, C. Caucheteur, Plasmonic optical fiber grating immunosensing: a review, Sensors 17 (2017) 1–19.
[27] H. Wang, X. Wang, J. Wang, W. Fu, C. Yao, A SPR biosensor based on signal amplification using antibody-QD conjugates for quantitative determination of multiple tumor markers, Sci. Rep. 6 (2016) 1–9, https://doi.org/10.1038/srep33140.
[28] J. Pollet, F. Delport, K.P.F. Janssen, K. Jans, G. Maes, H. Pfeiffer, M. Wevers, J. Lammertyn, Fiber optic SPR biosensing of DNA hybridization and DNA-protein interactions, Biosens. Bioelectron. 25 (2009) 864–869, https://doi.org/10.1016/j.bios.2009.08.045.
[29] V. Ranganathan, S. Srinivasan, A. Singh, M.C. DeRosa, An aptamer-based colorimetric lateral flow assay for the detection of human epidermal growth factor receptor 2 (HER2), Anal. Biochem. 588 (2020) 113471, https://doi.org/10.1016/j.ab.2019.113471.
[30] M. Loyez, C. Ribaut, C. Caucheteur, R. Wattiez, Functionalized gold electroless-plated optical fiber gratings for reliable surface biosensing, Sensor. Actuator. B Chem. 280 (2019) 54–61, https://doi.org/10.1016/j.snb.2018.09.115.
[31] S. Singh, R.K. Verma, B.D. Gupta, LED based fiber optic surface plasmon resonance sensor, Opt. Quant. Electron. 42 (2010) 15–28, https://doi.org/10.1007/s11082-010-9418-7.
[32] Y.S. Dwivedi, A.K. Sharma, B.D. Gupta, Influence of skew rays on the sensitivity and signal-to-noise ratio of a fiber-optic surface-plasmon-resonance sensor: a theoretical study, Appl. Optic. 46 (2007) 4563–4569, https://doi.org/10.1364/AO.46.004563.
[33] B.D. Gupta, S.K. Srivastava, R. Verma, Fiber Optic Sensors Based on Plasmonics, World Scie, WSPC, 2015.
[34] I. Arghir, F. Delport, D. Spasic, J. Lammertyn, Smart design of fiber optic surfaces for improved plasmonic biosensing, N. Biotech. 32 (2015) 473–484, https://doi.org/10.1016/j.nbt.2015.03.012.
[35] L.A. Obando, K.S. Booksh, Tuning dynamic range and sensitivity of plasmon resonance sensors, Anal. Chem. 71 (1999) 5116–5122.
[36] S. Ekgasit, C. Thammacharoen, F. Yu, W. Knoll, Influence of the metal film thickness on the sensitivity of surface plasmon resonance biosensors, Appl. Spectrosc. 59 (2005) 661–667.
[37] M. Iga, A. Seki, K. Watanabe, Gold thickness dependence of SPR-based hetero-core structured optical fiber sensor, Sensor. Actuator. B Chem. 106 (2005) 363–368, https://doi.org/10.1016/j.snb.2004.08.017.
[38] H. Suzuki, M. Sugimoto, Y. Matsui, J. Kondoh, Effects of gold film thickness on spectrum profile and sensitivity of a multimode-optical-fiber SPR sensor, Sensor. Actuator. B Chem. 132 (2008) 26–33, https://doi.org/10.1016/j.snb.2008.01.003.
[39] R. Zhang, S. Pu, X. Li, Gold-film-thickness dependent SPR refractive index and temperature sensing with hetero-core optical fiber structure, Sensors (2019) 19.
[40] E. Klantsataya, P. Jia, H. Ebendorff-Heidepriem, T.M. Monro, A. François, Plasmonic fiber optic refractometric sensors: from conventional architectures to recent design trends, Sensors (2017) 17, https://doi.org/10.3390/s17010012.
[41] D. Santano, I. Del Villar, I.R. Matias, Biosensors and Bioelectronics: X Trends in the design of wavelength-based optical fi bre biosensors (2008 – 2018), Biosens. Bioelectron. X. 1 (2019) 100015, https://doi.org/10.1016/j.biosx.2019.100015.
[42] F. Chiavaioli, C.A.J. Gouveia, P.A.S. Jorge, F. Baldini, Towards a uniform metrological assessment of grating-based optical fiber sensors: from refractometers to biosensors, Biosensors 7 (2017), https://doi.org/10.3390/bios7020023.